

PAPER • OPEN ACCESS

## Study of Temperature Field and Ampacity of 110kV AC Submarine Cables under Different Laying Conditions

To cite this article: Zhenxin Chen *et al* 2019 *J. Phys.: Conf. Ser.* **1346** 012037

View the [article online](#) for updates and enhancements.



**IOP | ebooks™**

Bringing you innovative digital publishing with leading voices to create your essential collection of books in STEM research.

Start exploring the collection - download the first chapter of every title for free.

# Study of Temperature Field and Ampacity of 110kV AC Submarine Cables under Different Laying Conditions

Zhenxin Chen<sup>1</sup>, Yanjie Le<sup>1,2</sup>, Heng Liu<sup>3\*</sup>, Fan Yang<sup>3</sup>, Wenkan Hu<sup>1</sup>, Kai Hu<sup>3</sup>, Jinxian Li<sup>3</sup> and Tingting He<sup>3</sup>

<sup>1</sup>Zhoushan Power Supply Company of State Grid Zhejiang Electric Power Company, Zhoushan, China

<sup>2</sup>Zhejiang Zhoushan Marine Power Research Institute Co., Ltd., Zhoushan, China

<sup>3</sup>State Key Laboratory of Power Transmission Equipment & System Security and New Technology, School of Electrical Engineering, Chongqing University, Chongqing, China

\*liuheng\_sw@cqu.edu.cn

**Abstract.** Submarine cables have complicated structures and high production process requirements. In order to make sure the submarine cables to operate safely and reliably, this paper takes into account how the different laying conditions of submarine cables affect the maximum allowable ampacity. A 110kV YJQ-1×500 XLPE submarine cable is taken as the research object, based on the finite element method, the electromagnetic-thermal coupling models of the submarine cable laying in underwater soil, seawater and pipeline is established respectively in Comsol Multiphysics to study their thermal field and ampacities. The results indicate that the laying conditions would affect the cables' heat dissipation, submarine cable lays in seawater has the highest ampacity and lays in the pipeline in landing section of the cable has the lowest ampacity. Moreover, the variation of temperature of seawater would also influence the ampacity of the submarine cable.

## 1. Introduction

In recent years, with the emphasis on environmental protection and renewable energy [1], clean energy power generation has been developed rapidly, one of the most important aspects is the offshore wind power generation which will drive more submarine cables to put into use [2-3]. Submarine cables are products with complex structures and extremely high requirements for manufacturing process, electrical and mechanical properties in power cables [4]. The different laying conditions of submarine cables is the main factor affects the maximum allowable ampacity of the submarine cables. Studying the variations of thermal field and maximum allowable ampacity of submarine cables under different laying conditions is of great significance to their safe and reliable operation.

At present, many scholars have devoted themselves to the research of thermal field and ampacity calculation of power cables. In [5], the transient temperature distribution and ampacity of underground power cable in tunnel has been established and calculated. In [6], they analysed the influence of different backfill materials on the ampacity of cables by using the finite element method, and proved that the calculation results are more reliable for non-standard direct buried installations. In [7], an equal proportion of buried cable test platform was built to test the influence of different types of soils on the heat transfer characteristics of the cable. The above papers mainly analyses the thermal field



and the ampacity of the AC terrestrial cables. The calculation methods are mostly based on the IEC-60287 standard [8-10] or the thermal field numerical analysis [11-12]. The study for the submarine cables is still in the early stages.

In this paper, a 110kV YJQ-1×500 XLPE submarine cable is taken as the research object, based on the finite element method, the electromagnetic-thermal coupling models of the submarine cable laying in underwater soil, seawater and pipeline are established respectively in Comsol Multiphysics to study their thermal field and ampacities. The influence of radial temperature distribution of submarine cables and the temperature of seawater upon on the ampacity of submarine cables also have been studied, which provided a reference and basis for the safe and reliable operation of the submarine cables.

## 2. Electromagnetic - thermal Coupling Model of 110 kV AC Submarine Cable

### 2.1. Electromagnetic Field Model of 110kV AC Submarine Cables

In order to simplify the mathematical model of the electromagnetic field of cables, the following assumptions are introduced:

1) Since the AC submarine cables operate at power frequency, the ratio of the conduction current density to the displacement current density is about  $10^7$ , so the effect of the displacement current can be neglected.

2) Submarine cable materials are the isotropic medium.

3) There is no free charge in the field.

Based on the above assumptions, the Maxwell equations can be simplified as:

$$\begin{cases} \nabla \times \mathbf{H} = \mathbf{J} \\ \nabla \times \mathbf{E} = -\frac{\partial \mathbf{B}}{\partial t} \\ \nabla \cdot \mathbf{B} = 0 \\ \nabla \cdot \mathbf{D} = 0 \end{cases} \quad (1)$$

Where,  $\mathbf{H}$  is magnetic field intensity,  $\mathbf{J}$  is conduction current density,  $\mathbf{E}$  is electric field intensity,  $\mathbf{B}$  is magnetic induction intensity,  $\mathbf{D}$  is electric displacement vector, and  $t$  is time.

The Magnetic potential vector  $\mathbf{A}$  meets  $\mathbf{B} = \nabla \times \mathbf{A}$ , brings the equation into the first and second equations of the Maxwell equations, and the excitation region for the external current source can be derived. The governing equation of  $\mathbf{A}$  is:

$$\left(\nabla \cdot \frac{1}{\mu} \nabla\right) \mathbf{A} = -\mathbf{J}_s + \sigma \frac{\partial \mathbf{A}}{\partial t} \quad (2)$$

For the non-current region, the governing equation of  $\mathbf{A}$  is:

$$\left(\nabla \cdot \frac{1}{\mu} \nabla\right) \mathbf{A} = 0 \quad (3)$$

Where,  $\mathbf{J}_s$  is source current density,  $\mu$  is magnetic permeability,  $\sigma$  is electronic conductivity. Solving the problem of electromagnetic field of AC submarine cables can be transformed into solving of Eq. (2) and (3), which must have definite solution and certain boundary conditions. The four common boundary conditions are:

1) The first boundary condition

Magnetic lines perpendicular to the boundary plane, that is,  $\mathbf{H}_t = 0$ , and is described by  $\mathbf{A}$ :

$$\begin{cases} \mathbf{n} \times \left(\frac{1}{\mu} \nabla \times \mathbf{A}\right) \Big|_{\Gamma_1} = 0 \\ \mathbf{n} \cdot \mathbf{A} \Big|_{\Gamma_1} = 0 \end{cases} \quad (4)$$

2) The second boundary condition

Magnetic lines parallel to the boundary plane, that is,  $\mathbf{B}_n=0$ , and is described by  $\mathbf{A}$ :

$$\begin{cases} \mathbf{n} \cdot (\nabla \times \mathbf{A})|_{\Gamma_2} = 0 \\ \mathbf{n} \times \mathbf{A}|_{\Gamma_2} = 0 \end{cases} \quad (5)$$

3) The third boundary condition

The boundary plane has a surface current density  $\delta_s$ , that is,  $\mathbf{n} \times \mathbf{H} = -\delta_s$ , and is described by  $\mathbf{A}$ :

$$\begin{cases} \mathbf{n} \times \left( \frac{1}{\mu} \nabla \times \mathbf{A} \right) |_{\Gamma_3} = -\delta_s \\ \mathbf{n} \cdot \mathbf{A}|_{\Gamma_3} = 0 \end{cases} \quad (6)$$

4) The fourth boundary condition

The specific value of  $\mathbf{A}$  on the boundary is given, the expression is as follow:

$$\mathbf{A}|_{\Gamma_4} = \mathbf{A}_0 \quad (7)$$

Where,  $\mathbf{n}$  is normal unit vector on the boundary,  $\Gamma$  is integral boundary.

## 2.2. Formatting author names

According to the Fourier's law and the law of conservation of energy, the governing equations which describes the thermal field of submarine AC cables can be obtained and expressed in Cartesian coordinates as:

$$\rho c \frac{\partial T}{\partial t} - \frac{\partial}{\partial x} \left( \lambda_x \frac{\partial T}{\partial x} \right) - \frac{\partial}{\partial y} \left( \lambda_y \frac{\partial T}{\partial y} \right) - \frac{\partial}{\partial z} \left( \lambda_z \frac{\partial T}{\partial z} \right) - Q_v = 0 \quad (8)$$

Where,  $\rho$  is density of the material,  $c$  is specific heat capacity of the material,  $T$  is temperature variable to be solved,  $\lambda_x$ ,  $\lambda_y$  and  $\lambda_z$  are the thermal conductivities of the material along the x, y and z directions respectively, for the isotropic materials, there is  $\lambda_x = \lambda_y = \lambda_z$ ,  $Q_v$  is heat source density.

According to the theory of heat transfer, the boundary conditions for solving the thermal field can be divided into three categories, the governing equations are:

$$\begin{cases} T|_{\Gamma_1} = T_0 \\ -\lambda \frac{\partial T}{\partial n} |_{\Gamma_2} = q_n \\ -\lambda \frac{\partial T}{\partial n} |_{\Gamma_3} = h(T_f - T_{amb}) \end{cases} \quad (9)$$

Where,  $q_n$  is heat flux density,  $h$  is convective heat transfer coefficient of the cable surface,  $T_f$  is temperature of cable surface,  $T_{amb}$  is ambient temperature.

According to the Stephen-Boltzmann law, the radiative heat dissipation boundary of the cables' surface can be expressed as:

$$-\lambda \frac{\partial T}{\partial n} = \sigma_0 \varepsilon (T_f^4 - T_{amb}^4) \quad (10)$$

Where,  $\sigma_0 = 5.67 \times 10^{-8}$  is Stefan-Boltzmann constant,  $\varepsilon$  is radiant heat dissipation rate of the cable surface.

### 2.3. Electromagnetic-thermal coupling effect of 110kV AC submarine cables

In solving the electromagnetic-thermal coupling problem, it is necessary to determine the unit volume heating rate of the heat source in the thermal field of cables and the heat flux density through the outer surface of the cables. For submarine cables, their electromagnetic loss includes conductor core loss, insulation loss, sheath and armour loss, et al. The main part of conductor loss is related to the conductivity of copper's core. The conductivity of copper and temperature is approximately linear, so the thermal field will in turn affect the electromagnetic losses of submarine cables. The coupling relationship between the electromagnetic field and thermal field of submarine cables are shown in Figure 1.

The relationship between electrical conductivity  $\sigma$  of the submarine cables' core and temperature  $T$  is:

$$\sigma = \frac{\sigma_{20}}{1 + \alpha(T - 20)} \quad (11)$$

Where,  $\sigma_{20}$  is conductivity of copper at 20°C,  $\alpha$  is temperature coefficient of conductivity of copper. After solving  $A$ , the current density  $\mathbf{J}$  at each cross section of the submarine cables and the electromagnetic loss density  $Q_v$  can be obtained as follows:

$$\mathbf{J} = \nabla \times \frac{1}{\mu} \nabla \times \mathbf{A} \quad (12)$$

$$Q_v = \frac{1}{\sigma} |\mathbf{J}|^2 \quad (13)$$

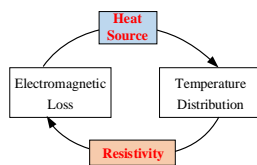


**Figure 1.** Electromagnetic-thermal Coupling Relationship of Submarine Cables

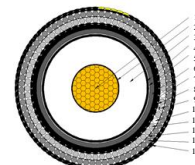


**Figure 2.** Structure of 110kV AC Submarine Cable

### 3. Calculation and Analysis of Thermal Field and Ampacities of 110kV AC Submarine Cables Under Different Laying Conditions

**Table 1.** Physical Structure Parameters 110kV AC Submarine Cables

Number	Name	Structure Size /mm	Nominal Diameter /mm	Number	Name	Structure Size /mm	Nominal Diameter /mm
1	Water-blocking Conductor	58×φ3.43	26.6	8	Inner Lining Layer	1.8	88.9
2	Conductor Shield	0.5+1.5	30.6	9	Optical Fibre Cable	2×φ6.0	-
3	Insulation	17	64.6	10	Cable Filling Layer	6.0	100.9
4	Insulation Shield	1.2	67.4	11	Alloy Wire	6×φ6.0	-
5	Water-blocking Buffer	2×0.5	69.9	12	Package Belt	2×0.3	-
6	Metal Sheath	2.7	75.3	13	Armoured Layer	52×φ6.0	113.8
7	Inner Sheath	5.0	85.3	14	Outer Ply	3.3	120.4±3.0

Submarine cables consist of a water-blocking conductor core, conductor shield, insulating layer, insulating shield, jacket layer, inner liner, armour layer and outer ply. Some high-voltage submarine cables even prefabricate the optical fiber cable. This paper takes a 110 kV YJQ-1×500 XLPE submarine cable as the research object, the model and the parameters of each part of the cable are shown in Table 1 and Figure 2.

### 3.1. Calculation and Analysis of Thermal Field and Ampacity of 110kV AC Submarine Cables Laying in Underwater Soil

3.1.1. *Laying parameters and meshing.* When the submarine cables are laying in underwater soil and the change of environmental factors along the submarine cable can be ignored, the only thing needs to be considered is the distribution of radial electromagnetic-thermal coupling field of the submarine cables. The laying parameters and model of submarine cables lay in underwater soil are shown in Table 2 and Figure 3. In this paper, the triangular element is used to mesh the submarine cables in finite element method. The meshing result is shown in Figure 4.

**Table 2.** Laying Parameters of AC Submarine Cables Lay in Underwater Soil

Laying Parameters	Value
Heat Transfer Coefficient of Sea Water/( W/(m <sup>2</sup> ·K))	400
Seabed Soil Resistivity/(Ω·m)	0.58×10 <sup>8</sup>
Relative Conductivity of Underwater Soil	1
Relative Permeability of Underwater Soil	1
Thermal Conductivity of Underwater Soil	1
Buried Depth/m	2
Horizontal Spacing of Submarine Cables/m	0.3
Temperature of Underwater Soil/K	293.15

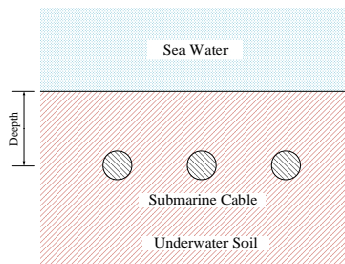


**Figure 3.** 110kV AC Submarine Cables Laying in Underwater Soil

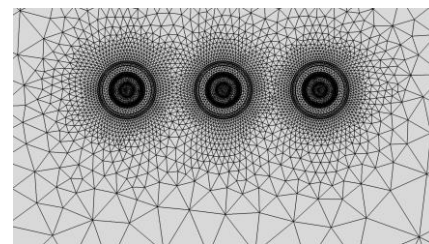


**Figure 4.** Meshing Result of Submarine Cable Laying in Underwater Soil

3.1.2. *Results and Analysis.* Due to the electromagnetic induction effect and location distribution of mesophase is not conducive to heat dissipation, its temperature is the highest. When the temperature of mesophase reaches 363.15K, the iterative calculation ends and the ampacity of corresponding three-phase submarine cable which lays in underwater soil is 900A. At the same time, the temperature of other two-phase core is 359.98K and 359.93K respectively. The temperature difference between the three-phase submarine cable is about 3.2K. The temperature distribution of 110kV three-phase submarine cables, the global temperature distribution and the isotherm distribution are shown in Figure 5-7 respectively.

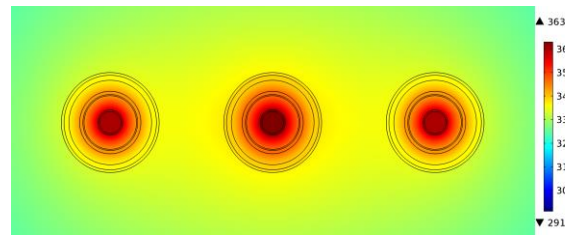


**Figure 5.** Temperature Distribution of 110kV AC Three-phase Submarine Cables Lay in Underwater Soil

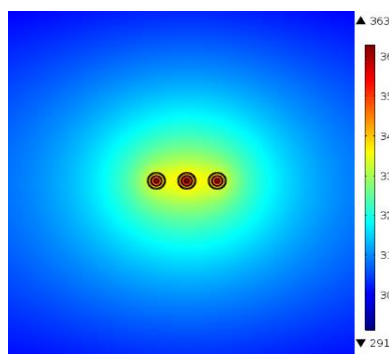


**Figure 6.** Global Temperature Distribution of 110kV AC Three-phase Submarine Cables Lay in Underwater Soil

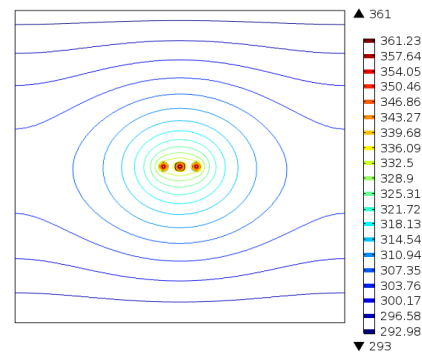


**Figure 7.** Isothermal Distribution of 110kV AC Three-phase Submarine Cables Lay in Underwater Soil

As can be seen from the above figures, the temperature of mesophase is the highest, and the heat is conducted outward from the core of cables. The isotherms are distributed in an elliptical shape under the influence of the thermal conductivity of the soil. The density decreases from the inside to outside. The temperature near the cable declines rapidly and it declines more slowly away from the cable.

Take a further research to the radial temperature distribution of the middle phase of submarine cables, the radial temperature distribution curve of the middle phase is shown in Figure 8.

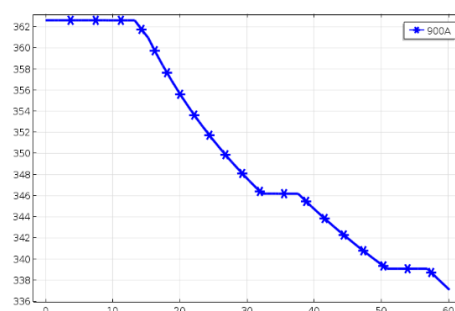


**Figure 8.** Radial Temperature Distribution Curve of the Middle Phase

It can be seen from the multi-layer structure of the submarine cable that thermal conductivity of the cable's core is  $400\text{W}\cdot(\text{m}\cdot\text{K})^{-1}$  and the temperature distribution is uniform which value is 363.15K. The thickness of the conductor shield is thin, which closely attaches to the conductor, its thermal conductivity is  $0.48\text{W}\cdot(\text{m}\cdot\text{K})^{-1}$  and temperature is approximately equal to the temperature of conductor metal. The thermal conductivity of the insulation layer is  $0.286\text{W}\cdot(\text{m}\cdot\text{K})^{-1}$  and the thickness of it is the thickest, which conduct the heat slowly, so the temperature declines rapidly from 362.77K to 350.64K, the temperature difference reaches 12.13K. The thickness of the inner lining layer is large, and its thermal conductivity is relatively small, so the temperature declines fast, and the temperature

difference is 5.42K. The material of armored layer is galvanized steel wire, which thickness is small, thermal conductivity is relatively large, and the temperature is almost unchanged at 345.15K. The thermal conductivity of the outer ply is small, which causes the heat conduction slowly, the temperature of it is 343.12K, and the temperature difference between the conductor core is 20.03K.

### 3.2. Calculation and Analysis of Thermal Field and Ampacity of 110kV AC Submarine Cables Lay in Seawater

3.2.1. *Laying parameters and meshing.* Submarine cables are usually laid about 2 meters under the seabed. But the laying environment of submarine cables is complex and changeable, Due to fluctuations of seabed, trenches and other reasons, the submarine cables also lay in seawater. The laying parameters and model of submarine cables lay in seawater are shown in Table 3 and Figure 9.

**Table 3.** Environmental Parameters of AC Submarine Cables Lay in Seawater

Laying Parameters	Value
Heat Transfer Coefficient of Sea Water/( W/(m <sup>2</sup> ·K))	400
Horizontal Spacing of Submarine Cables/m	0.3
Temperature of Seawater/K	303.15

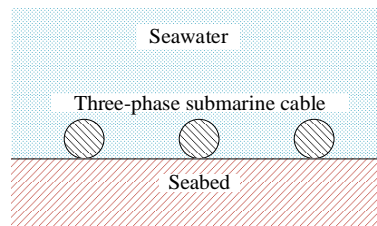


**Figure 9.** 110kV AC Submarine Cables Lay in Seawater

Because of the effect of convection heat transfer is far better than the thermal conductivity of seabed, the heat transfer of seabed can be ignored. The meshing method adopted is the same as in Section 3.1.1 and will not be repeated here.

3.2.2. *Results and Analysis.* When the temperature of seawater is 303.15K, the temperature distribution of the three-phase submarine cable is shown in Figure 10. At the same time, the temperature of the cable's core reaches 363.15K, and the effective value of the ampacity is calculated as 1535A. The corresponding relationship between the temperature of seawater and the ampacity is obtained through simulation. The results are shown in Table 4. As can be seen, when the temperature of seawater increases, the ampacity will continue to decrease.

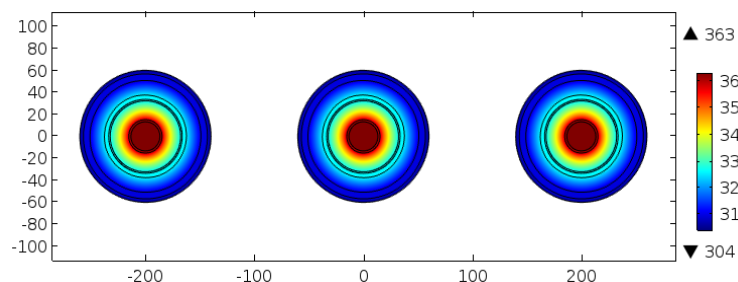


**Figure 10.** Temperature Distribution of Submarine Cables Lay in Seawater

**Table 4.** Relationship of the Temperature of Seawater and the Ampacity of 110kV AC Submarine Cables

Temperature of Seawater/K	Value of Ampacity
273.15	1878
278.15	1825
283.15	1771
288.15	1715
293.15	1657
298.15	1597
303.15	1535

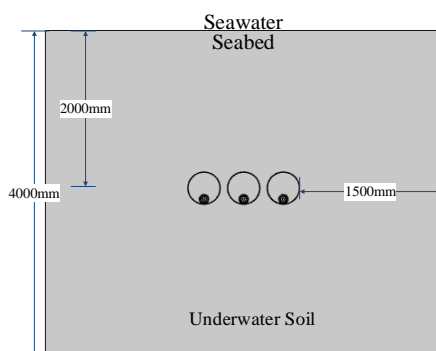
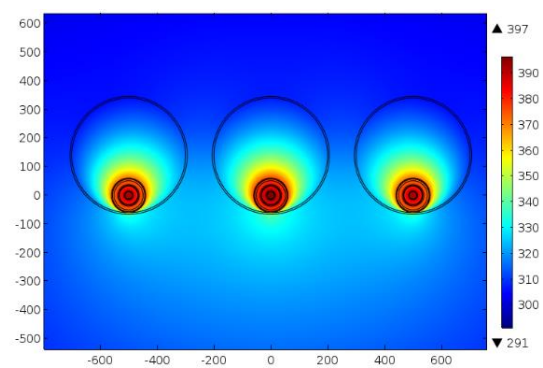
### 3.3. Calculation and Analysis of Thermal Field and Ampacity of 110kV AC Submarine Cables Lay in Pipeline

**3.3.1. Laying parameters and meshing.** The landing section of submarine cables lay in pipeline can enhance the protection of the cables. Because of the air in the pipeline, the radiant heat transfer of the outer surface of the cable and cooling effect is not good as lay in the underwater soil. It is necessary to calculate and analysis the thermal field and ampacity of 110kV AC submarine cables lay in pipeline.

The 1×3 PVC pipeline is selected, the laying parameters and model of landing section of submarine cables lay in pipeline are shown in Table 5 and Figure 11. The meshing method adopted is the same as in Section 3.1.1 and will not be repeated here.

**Table 5.** Laying Parameters of AC Submarine Cables Laying in Pipeline of Landing Section

Laying Parameters	Value
Diameter of Pipeline/m	0.4
Thickness of Pipeline/m	0.0005
Fluid in the Pipeline	Air
Thermal Conductivity of Pipeline	0.1667
Thermal Conductivity of Soil	1
Depth of Laying/m	2
Temperature of Soil/K	293.15
Temperature of Seawater/K	291.15

**Figure 11.** The landing section of 110kV AC Submarine Cables Lay in Pipeline**Figure 12.** Temperature Distribution of Landing Section Submarine Cables Lay in Pipeline

*3.3.2. Results and Analysis.* When the ampacity is 900A, the maximum temperature appears in the middle phase, reaches 396.51K, and it exceeds the maximum allowable temperature 33K. Laying in pipeline not only is the weakness of heat dissipation for submarine cables, but also limit the ampacity of submarine cable. The temperature distribution of submarine cables when the ampacity reaches 900A is shown in Figure 12.

From the above results, it can be seen that the maximum temperature of laying in pipeline is 33.36K higher than that laying in the underwater soil. This is because the natural air convection in the pipeline is very weak and limited for heat transfer which mainly depends on the radiation on the inner wall of the pipeline and the outer surface of the submarine cable. The efficiency of radiative heat transfer is lower than that of laying in underwater soil, so the heat dissipates weakly, and it gathers in the body of submarine cables, the temperature of the conductor's core rises obviously.

When the temperature of the middle phase of the submarine cable's core reaches 363.15K, the calculation of the ampacity obtained by iteration is 740A, compared with the situation of laying in underwater soil and seawater, the ampacity decreases by 17.78% and 107.43%.

#### 4. Conclusions

1) When the temperature of submarine cables lay in underwater soil, seawater and pipeline reaches 363.15K, the ampacity is 900A, 1535A and 740A respectively. The ampacity of laying in pipeline decreases by 17.78% and 107.43% respectively compared with the other two situations.

2) When the submarine cable is laying in underwater soil, the radial temperature distribution of the submarine cable is decreased from the inside to the outside, and the temperature difference between them is as high as 20.03K.

3) The ampacity of submarine cable lay in seawater decreases with the temperature of seawater increases. Therefore, during the calculation of submarine cables' ampacity, it is necessary to check the maximum seawater temperature of summer over years and make reasonable choices.

#### Acknowledgements

The authors acknowledge the support of the National Key Research and Development Program of China (2016YFB0900704) and the Science and Technology Project of SGCC (5211011600LF).

#### References

- [1] Benato, R., Sessa, S, D., Forzan, M., et al.: 'Finite Element model of a 3m long three-core armoured submarine cable'. Aeit International Conference. Capri, Italy, Oct 2017, pp. 1-6
- [2] Herry, Nugraha., Zivion, O, Silalahi., Ngapuli, I, Sinisuka.: 'Maintenance Decision Models for Java-Bali 150-kV Power Transmission Submarine Cable Using RAMS', IEEE Power and Energy Technology Systems Journal, 2016, 3, (1), pp. 24-31
- [3] Marzinotto, M.: 'Extruded Cables for High-Voltage Direct-Current Transmission - Advances in Research and Development', Wiley & Sons, 2013
- [4] Bawart, M., Marzinotto, M., Mazzanti, G.: 'Diagnosis and location of faults in submarine power cables', IEEE Electrical Insulation Magazine, 2016, 32, (4), pp. 34-37
- [5] Liang, Y.: 'Transient temperature analysis and short-term ampacity calculation of power cables in tunnel using SUPG finite element method'. Industry Applications Society Annual Meeting. Lake Buena Vista, FL, USA, Oct 2013, pp. 1-4
- [6] Leon, F, D., Anders, G, J.: 'Effects of Backfilling on Cable Ampacity Analyzed With the Finite Element Method', IEEE Transactions on Power Delivery, 2008, 23, (2), pp. 537-543
- [7] Vollaro, R, D, L., Fontana, L.: 'Vallati A. Experimental study of thermal field deriving from an underground electrical power cable buried in non-homogeneous soils', Applied Thermal Engineering, 2014, 62, (2), pp. 390-397
- [8] IEC60287-1: 'Calculation of the current rating-part 1-1: current rating equations(100% load factor) and calculation of losses ', 2014
- [9] IEC60287-2: 'Calculation of the current rating-part 2-1: thermal resistance', 2015

- [10] IEC60287-3: 'Calculation of the current rating-part 3-1: sections on operating conditions', 2017
- [11] Olsen, R., Anders, G. J., Holboell, J., et al.: 'Modelling of Dynamic Transmission Cable Temperature Considering Soil-Specific Heat, Thermal Resistivity, and Precipitation', IEEE Transactions on Power Delivery, 2013, 28, (3), pp. 1909-1917
- [12] Meng, X. K., Wang, Z. Q., Li, G. F.: 'Dynamic Analysis of Core Temperature of Low-Voltage Power Cable Based on Thermal Conductivity', Canadian Journal of Electrical & Computer Engineering, 2016, 39, (1), pp. 59-65.